Portfolio Decisions and Brain Reactions via the CEAD Method

Wolfgang K. Härdle
Hauke R. Heekeren
Piotr Majer
Peter N.C. Mohr

C.A.S.E. Center for Applied Statistics and Economics
Humboldt-Universität zu Berlin
Freie Universität Berlin
http://lvb.wiwi.hu-berlin.de
http://www.ewi-psy.fu-berlin.de
http://www.case.hu-berlin.de

Investments and Brain Correlates

- Which part of brain is activated during *investment decisions* ?
- Is risk attitude reflected in brain activity?

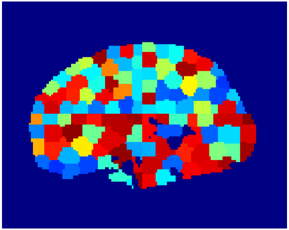

ID Experiment

- Survey by Department of Education and Psychology, FU Berlin
- 19 healthy volunteers ▸ payoff

- Investment Decision (ID) task ($\times$256)
  safe vs. **random** (μ, σ) ▸ return
- fMRI images: 2 sec$\times$1400 $\approx$ 48 min
- Can one identify brain reactions?

Investment Decision

Choose between:

A) **Safe**, fixed return 5%

B) **Random**, investment return (3 types)

- Single Investment
- Portfolio of 2 (perfectly) correlated investments
- Portfolio of 2 uncorrelated investments

- Each type of portfolio $\times 64$, single $\times 128$
- Display and decision time: 7 sec; Answers

ID Experiment

Figure 1: Decide between **A)** 5% return and displayed **B)** portfolio/investment.

fMRI

- functional Magnetic Resonance Imaging

- Measuring Blood Oxygenation Level Dependent (BOLD) effect every 2 sec
  High-dimensional, high frequency & large data set

fMRI

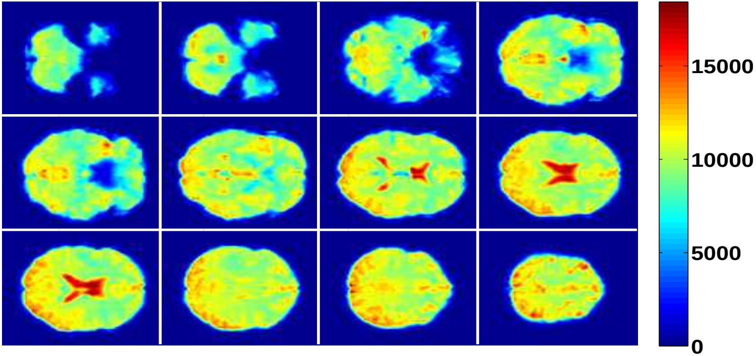

Figure 2: fMRI image observed every 2 sec, 12 horizontal slices of the brain's scan, $91 \times 109 \times 91 (x, y, z)$ data points of size 22 MB; voxel resolution: $2 \times 2 \times 2mm^3$

fMRI Dynamics ▸ fMRI methods

Hemodynamic response (1 voxel) ▸ HRF

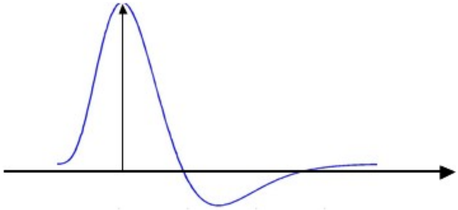

- Is there a significant reaction to specific stimuli?
- Which brain regions are activated?

fMRI Analysis: CEAD Method

C -luster
- fundamental units: spatially contiguous groups of voxels

E -stimation
- extract common signal vs. noise

A -ctivation
- smaller number of hypotheses tests
- signal easier to detect

D -ecision
- model-free analysis of cluster dynamics

Risk Perception – Thermodynamics

Theoretical framework

- Risk-return model
  Mohr et al., 2010

- Mechanical Equivalent of Heat
  1st law of thermodynamics
  Mayer, 1841

Empirical evidence

- fMRI analysis

- Experiments "Joule apparatus"
  Joule, 1843

Outline

1. Motivation ✓
2. fMRI Clustering
3. DSFM
4. Risk Attitude
5. Empirical results
6. Appendix

Clustering

- Find clusters (groups of voxels)
- A cluster has to be contiguous and homogeneous
- Data-driven (size,shape)
- Differences between clusters should be as large as possible

Proximity measure and group-building algorithm for fMRI?

Proximity between Voxels

▸ Correlation

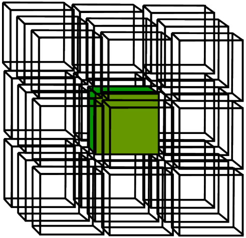

- $Y_{t,j}$ - BOLD signal observed at voxel j with $3D$ coordinates $X_j = (x_j, y_j, z_j)$, $j = 1, \ldots, J$
- Proximity measure $w(j,k)$ between Y_j and Y_k

$$w(j,k) = \begin{cases} \max\{\mathrm{Corr}_t(Y_j, Y_k), 0\}, & \text{for } \|X_j - X_k\| < \mathbf{d} \\ 0, & \text{otherwise} \end{cases}$$

d - fixed distance, such that $\{\tilde{u} : \|X_{\tilde{u}} - X_k\| < d\}$ is a $3D$ neighborhood ($3\sqrt{3}$mm); Corr_t - Pearson correlation over 2×1400

Cut Cost and Normalized Cut

- Cost of partitioning $\mathcal{Y}$ into P and Q groups, $\mathcal{Y} = P + Q$

$$Cut(P,Q) = \sum_{Y_j \in P, Y_k \in Q} w(j,k)$$

sum of all "neglected" similarities between voxels in P and Q

minimizing the cut cost: singletons

- Normalized cut:

$$N_{cut}(P,Q) = \frac{cut(P,Q)}{\sum_{Y_j \in P, Y_k \in \mathcal{Y}} w(j,k)} + \frac{cut(P,Q)}{\sum_{Y_j \in Q, Y_k \in \mathcal{Y}} w(j,k)}$$

Normalized cut (NCUT) spectral clustering

Hierarchically divide $\mathcal{Y}$ into pre-specified number of clusters K (top-down):

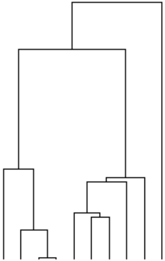

1. Find the division P^* and Q^*,
   $$(P^*, Q^*) = \underset{Y=P+Q}{\operatorname{argmin}} N_{cut}(P, Q)$$
2. Decide if the current partition should be subdivided
3. Recursively partition the segmented parts, if necessary

Notation

$$\underbrace{(X_{1,1}, Y_{1,1}), \ldots, (X_{J,1}, Y_{J,1})}_{t=1}, \ldots, \underbrace{(X_{1,T}, Y_{1,T}), \ldots, (X_{J,T}, Y_{J,T})}_{t=T},$$

$X_{j,t} \in \mathbb{R}^d, \; Y_{j,t} \in \mathbb{R}$
T - the number of observed time periods
J - the number of the observations in a period t
$\mathrm{E}(Y_t|X_t) = F_t(X_t)$

Quantify $F_t(X_t)$. How does it move?

Dynamic Semiparametric Factor Model

$$\mathrm{E}(Y_t|X_t) = \sum_{l=0}^{L} Z_{t,l} m_l(X_t) = Z_t^\top m(X_t) = Z_t^\top A^* \Psi$$

$$\begin{aligned}
Z_t &= (\mathbf{1}, Z_{t,1}, \ldots, Z_{t,L})^\top \text{low dim (stationary) time series} \\
m &= (m_0, m_1, \ldots, m_L)^\top, \text{tuple of functions} \\
\Psi &= \{\psi_1(X_t), \ldots, \psi_K(X_t)\}^\top, \psi_k(x) \text{ space basis} \\
A^* &: (L+1) \times K \text{ coefficient matrix}
\end{aligned}$$

DSFM Estimation

$$Y_{t,j} = \sum_{l=0}^{L} Z_{t,l} m_l(X_{t,j}) + \varepsilon_{t,j} = Z_t^\top A^* \psi(X_{t,j}) + \varepsilon_{t,j}$$

- $\psi(x) = \{\psi_1(x), \ldots, \psi_K(x)\}^\top$ tensor B-spline basis

$$(\widehat{Z}_t, \widehat{A^*}) = \arg \min_{Z_t, A^*} \sum_{t=1}^{T} \sum_{j=1}^{J} \left\{ Y_{t,j} - Z_t^\top A^* \psi(X_{t,j}) \right\}^2 \qquad (1)$$

- Minimization by Newton-Raphson algorithm

B-Splines

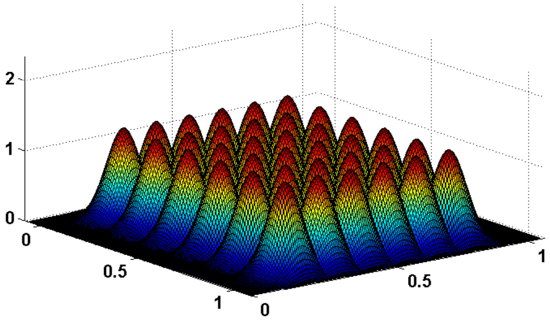

Figure 3: B-splines basis functions; order of B-splines: quadratic; number of knots: $6 \times 6 = 36$ ▸ B-Splines

Risk Attitude

- Risk-return choice model

$$V_r^i = \overline{x}_r - \beta_i S_r, \quad 1 \le i \le n, 1 \le r \le 256$$

x_r - portfolio return stream, $\overline{x}_r$ - average return (μ)
S_r - standard deviation of x_r (σ risk)
V_r^i - subjective value (unobserved), 5% - risk free return

- β Risk attitude parameter

Risk Attitude

- Estimation of individual risk attitude by logistic regression

$$
\begin{aligned}
\mathrm{P}\{\text{risky choice}|x\} &= \frac{1}{1+\exp\{\overline{x}-\beta S(x)-5\}} \\
\mathrm{P}\{\text{sure choice}|x\} &= 1-\frac{1}{1+\exp\{\overline{x}-\beta S(x)-5\}}
\end{aligned}
$$

risky choice - unknown return, sure choice - fixed, 5% return

- $\widehat{\beta}$ estimated by maximum likelihood

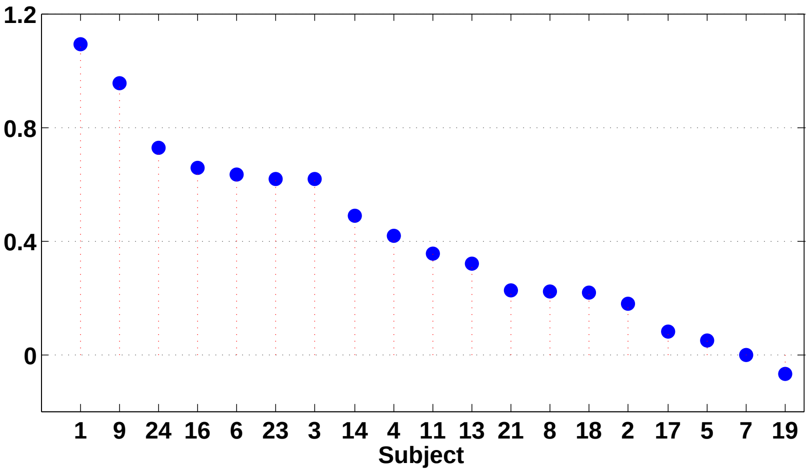

Figure 4: Risk attitude $\widehat{\beta}_i$ for 19 subjects.

Empirical Results: Clustering

- Number of clusters: 1000; cluster index $\mathfrak{s}$, $\mathfrak{s} = 1, \ldots, 1000$
  - 200: interpretability (anatomical atlases i.e. Talairach)
  - 1000: more accurate functional connectivity patterns

min	max	mean	median	Total
1	353	207.4	208	1000

Table 1: Descriptive statistics of clustering results averaged over subjects.

Computational time: 19×30 hours

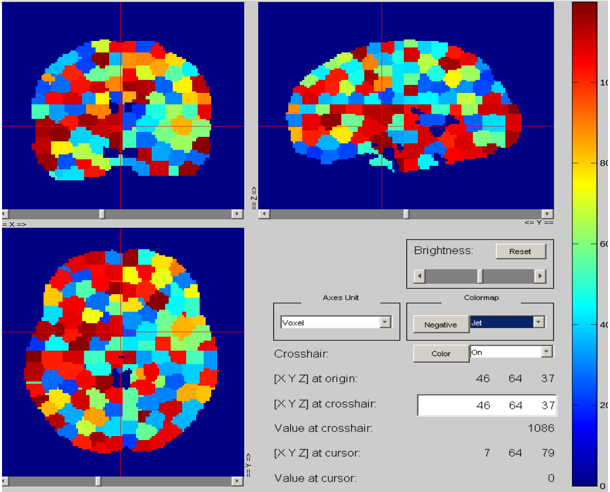

Figure 5: Parcellation results for the 1st subject's brain into 1000 clusters by NCut algorithm.

Cluster Activation

Heller et al. (2006): average over voxels in the cluster $\mathfrak{s}$ and test for activation

- Advanced dimension reduction technique: DSFM ▸ Simulations
  applied separately to each cluster $\mathfrak{s}$
- $Y_{t,I_\mathfrak{s}} = Z_t^\top m(X_{t,I_\mathfrak{s}}) + \varepsilon_{t,I_\mathfrak{s}}$ ▸ Residual Analysis
  $Y_{t,I_\mathfrak{s}}$ - BOLD; $X_{I_\mathfrak{s}}$ - voxel's coordinates; $I_\mathfrak{s} = \{j : j \in \mathfrak{s}\}$
- Cluster dynamics represented by low-dimensional factor loadings

Figure 6: Middle Horizontal slice of DSFM-clustered Brain scans of subject 1 observed over entire experiment (1400 scans). Each cluster is modeled with 1 dynamic factor, $\widehat{Z}_t$ are demeaned and standardized; number of clusters: 1000.

Cluster Activation

- First-level analysis:

  Testing the trigger events for estimated univariate $\widehat{Z}_t$ ▸ GLM

  - design matrix: convolution of stimulus and double Gamma HRF
  - active clusters selected by *z-scores*

- Group analysis by ▸ mixed-effects model

Cluster Activation: DMPFC

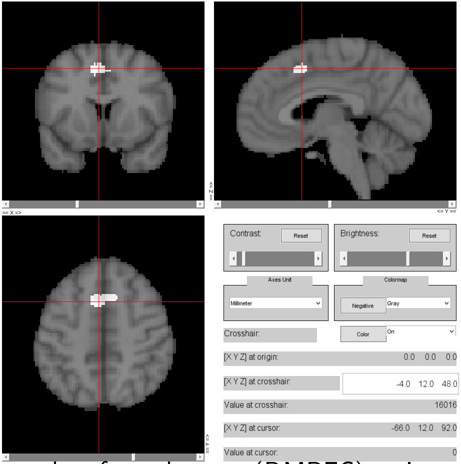

Figure 7: Dorsolateral prefrontal cortex (DMPFC) activated during all type of investment decisions in the group-level analysis. (▸ Z-scores)

Cluster Activation: aINS

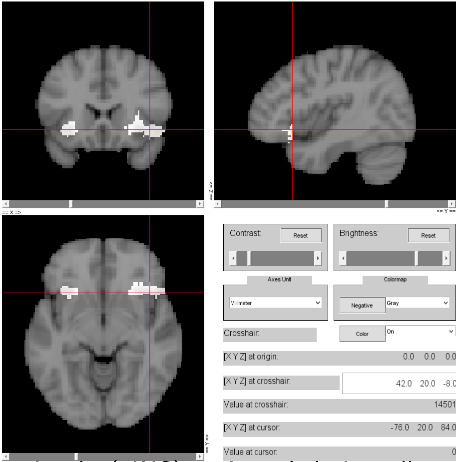

Figure 8: Anterior insula (aINS) activated during all type of investment decisions in the group-level analysis. ▸ Z-scores, ▸ aINS(l) ▸ aINS(r)

Estimated Factor Loading: DMPFC, ▸ ACF

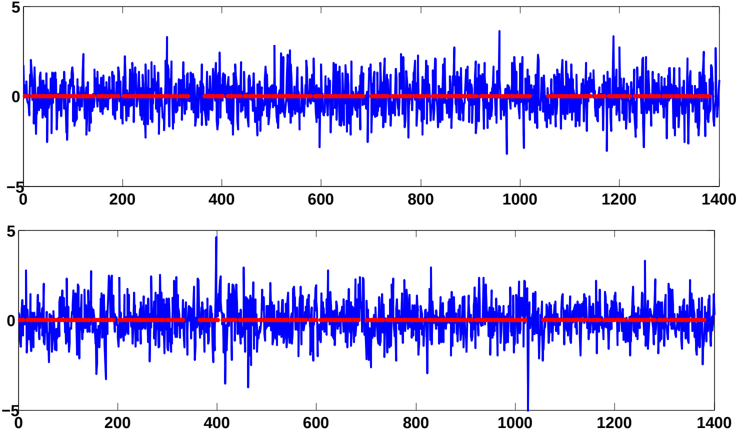

Figure 9: Estimated **DMPFC** $\widehat{Z}$ for subject 1 (top) and 19 (bottom); red dots denote stimulus.

Estimated Factor Loading: aINS, ACF

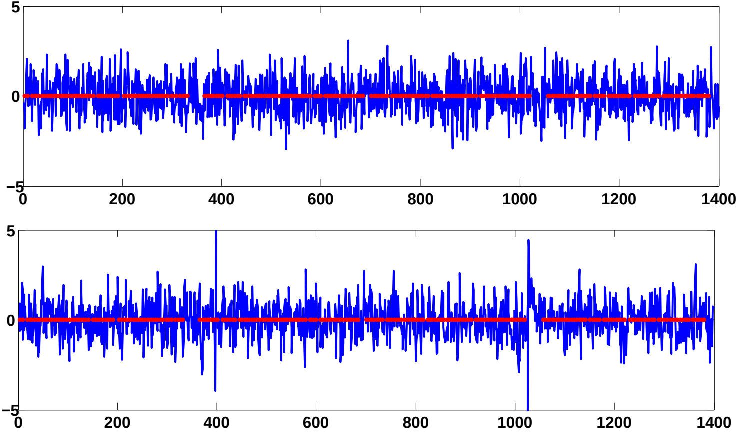

Figure 10: Estimated **aINS**(left) $\widehat{Z}$ for subject 1 (top) and 19 (bottom); red dots denote stimulus.

Estimated Factor Loading: aINS, ACF

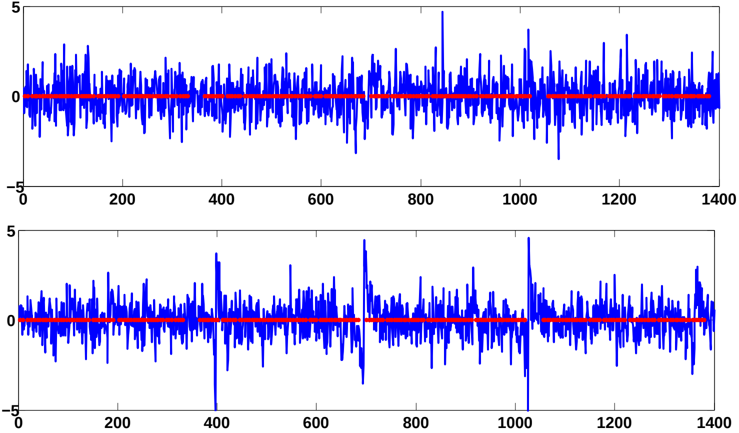

Figure 11: Estimated **aINS**(right) $\widehat{Z}$ for subject 1 (top) and 19 (bottom); red dots denote stimulus.

Risk attitude / Stimulus Response

- **ID**-related activated clusters: **aINS** (left, right), **DMPFC**
- Average reaction to r stimulus (up to 8 seconds after)
  $\Delta \widehat{Z}^i_r = \frac{1}{4} \sum_{\tau=1}^{4} \widehat{Z}^i_{r+\tau} - \widehat{Z}^i_r$
- Average reaction to stimulus: $\overline{\Delta} \widehat{Z}^i = \frac{1}{256} \sum_{r=1}^{256} \Delta \widehat{Z}^i_r$

Risk attitude / Stimulus Response

$$\beta^i = C + \alpha_1 \cdot \overline{\Delta}\widehat{Z}^i_{DMPFC} + \alpha_2 \cdot \overline{\Delta}\widehat{Z}^i_{aINS(l)} + \alpha_3 \cdot \overline{\Delta}\widehat{Z}^i_{aINS(r)} + \varepsilon^i \quad (2)$$

	Estimate	SE	tStat	pValue
C	0.097	0.115	0.861	0.403
$\overline{\Delta}\widehat{Z}_{DMPFC}$	0.851	0.526	1.619	0.126
$\overline{\Delta}\widehat{Z}_{aINS(r)}$	-1.506	0.550	-2.737	0.015
$\overline{\Delta}\widehat{Z}_{aINS(l)}$	-1.126	0.379	-2.967	0.001

Table 2: Risk attitude regressed on the average response; $R^2 = 0.47$, adj.$R^2 = 0.36$.

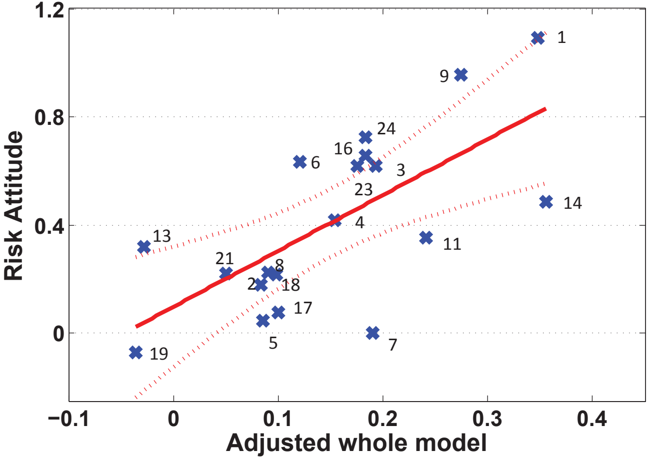

Figure 12: Added variable plot for model given in (2). Horizontal axis denotes the (rescaled) best linear combination of regressors $\overline{\Delta}\widehat{Z}$ that fit β.

$$\beta^i = \alpha_2 \cdot \overline{\Delta}\widehat{Z}^i_{aINS(l)} + \alpha_3 \cdot \overline{\Delta}\widehat{Z}^i_{aINS(r)} + \varepsilon^i \quad (3)$$

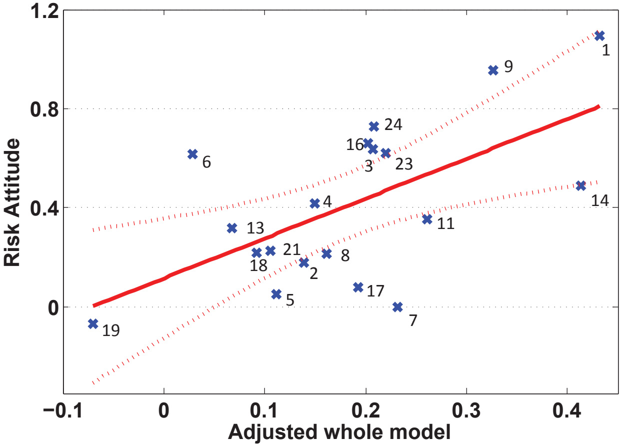

Figure 13: Added variable plot for the model (3); $R^2 = 0.37$, adj. $R^2 = 0.30$, p-value: 0.03, 0.02 for $\overline{\Delta}\widehat{Z}_{aINS(r)}$ and $\overline{\Delta}\widehat{Z}_{aINS(l)}$, respectively.

Risk attitude / Stimulus Response

- Exclude i observation and reestimate the model (3)
- Predict β^i by $\overline{\Delta}\widehat{Z}^i_{aINS(l)}$ and $\overline{\Delta}\widehat{Z}^i_{aINS(r)}$

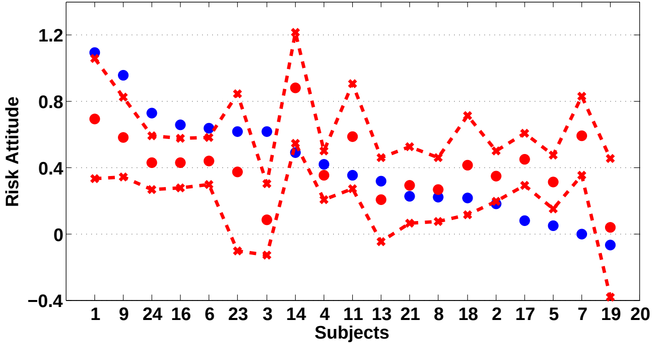

Figure 14: Risk attitude β^i (blue dots), predicted $\widetilde{\beta}^i$ (red dots) and 95% prediction confidence intervals (dashed line) for all 19 subjects.

- Weighted average reaction: $\Delta_w \widehat{Z}_r^i = \sum_{\tau=1}^{4} w_\tau (\widehat{Z}_{r+\tau}^i - \widehat{Z}_r^i)$, $\sum_{\tau=1}^{4} w_\tau = 1$

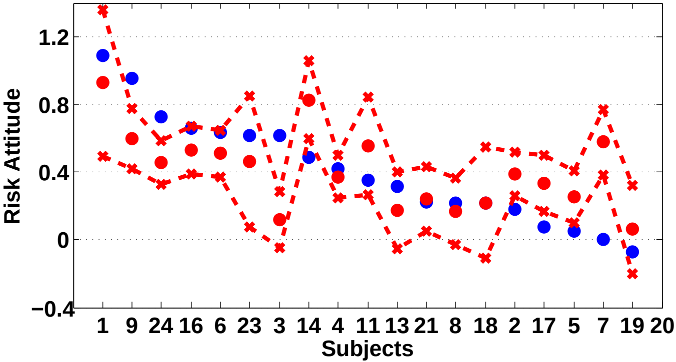

Figure 15: Risk attitude β^i (blue dots), predicted $\widetilde{\beta}^i$ (red dots) and 95% prediction confidence intervals (dashed line) for all 19 subjects for weighted average reaction to stimulus; ▸ Weight derivation $w = [.38\ .41\ .16\ .05]$; mean prediction error: 0.2.

Conclusion

- Local dynamic representation of the brain data
- Activation results similar to the GLM method
- Risk attitude attributed to aINS
- Risk attitude successfully predicted based on fMRI data

Portfolio Decisions and Brain Reactions via the CEAD Method

Wolfgang K. Härdle
Hauke R. Heekeren
Piotr Majer
Peter N.C. Mohr

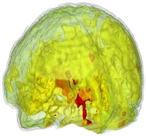

C.A.S.E. Center for Applied Statistics and Economics
Humboldt-Universität zu Berlin
Freie Universität Berlin
http://lvb.wiwi.hu-berlin.de
http://www.ewi-psy.fu-berlin.de
http://www.case.hu-berlin.de

References

- van Bömmel, A., Song, S., Majer, P., Mohr, P.,Heekeren, H., Härdle, W.
  Risk Patterns and Correlated Brain Activities. Multidimensional Statistical Analysis of fMRI Data in Economic Decision Making Study
  Psychometrika, doi:10.1007/s11336-013-9352-2, 2013.

- Heller, R., Stanley D., Yekutieli, D., Rubin, N., Benjamini, Y.
  Cluster-based analysis of FMRI data
  NeuroImage, 33: 599-608, 2006.

- Mohr, P., Biele G., Krugel, L., Li S., Heekeren, H.
  Neural foundations of risk-return trade-off in investment decisions
  NeuroImage, 49: 2556-2563, 2010.

References

Park, B., Mammen, E., Härdle, W. and Borak, S.
Time Series Modelling with Semiparametric Factor Dynamics
J. Amer. Stat. Assoc., 104(485): 284-298, 2009.

Ramsay, J. O. and Silverman, B. W.
Functional Data Analysis
New York: Springer, 1997.

Shi, J. and Malik, J.
Normalized cuts and image segmentation.
IEEE Trans. on P. Anal. and Mach. Int., 22: 888–905, 2000.

References

Woolrich, M., Ripley, B., Brady, M., Smith, S.
Temporal Autocorrelation in Univariate Linear Modelling of FMRI Data
NeuroImage, 21: 2245-2278, 2010

Talairach, J. and Tournoux, P.
Co-Planar Stereotaxic Atlas of the Human Brain
Thieme, 2008.

fMRI Methods

fMRI Dynamics

- Voxel-wise GLM Voxel-wise GLM
  - linear model for each voxel separately
  - strong a priori hypothesis
- Tensor probabilistic independent component analysis (T-PICA)
  - factors in spatial, temporal and subject domain
- Dynamic Semiparametric Factor Model (DSFM)
  - Use a "time & space" dynamic approach
  - Low dim time series exploratory analysis

Voxel-wise GLM fMRI methods, Cluster Activation, Simulations

- FEAT - FMRI Expert Analysis Tool by Department of Clinical Neurology, University of Oxford

- GLM framework

$$Y = X\mathfrak{b} + \eta, \tag{4}$$

  Y - single voxel BOLD time series, X - design matrix (predicted response to stimulus i.e. **ID**, visual, auditory), $\mathfrak{b}$ - effect size

- Significant, active areas ($\mathfrak{b} >> 0$) selected by *z-scores*$\equiv \frac{\mathfrak{b}_i - 0}{\sqrt{\mathrm{Var}(\mathfrak{b}_i)}}$ and grouping (i.e. 20 neighbors) scheme

HRF

▸ fMRI methods ▸ fMRI dynamics

- Hemodynamic response function e.g. Double Gamma function

$$h(t) = \left(\frac{t}{5.4}\right)^6 \exp\left(-\frac{t-5.4}{0.9}\right) - 0.35\left(\frac{t}{10.8}\right)^{12} \exp\left(-\frac{t-10.8}{0.9}\right),\ t \geq 0\text{-time [sec]}$$

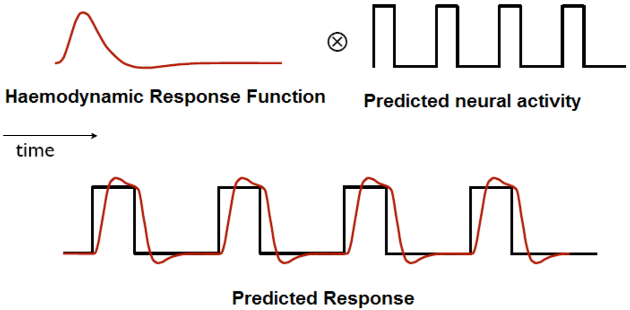

Figure 16: Predicted response as a convolution of a stimulus signal and a HRF. Figure modified from FEAT - FMRI.

Design Matrix

▸ fMRI methods

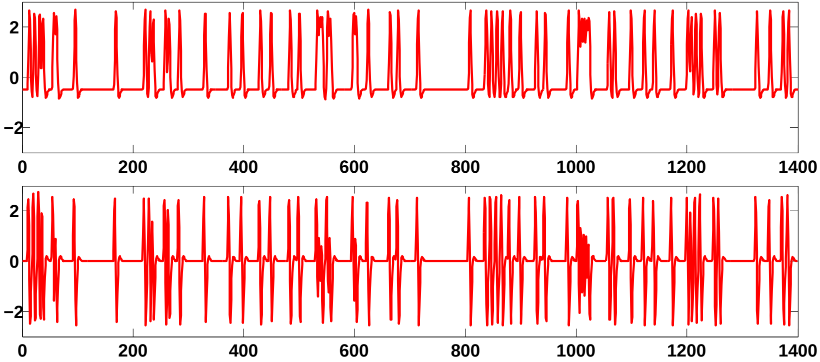

Figure 17: Predicted reaction to the stimulus (upper panel) and its derivative (lower panel) as an example of the elements of design matrix X 4).

Mixed-effects Model

▸ Cluster Activation

Higher-level analysis based on the Voxel-wise GLM input:

- $Y^i_j = X\mathfrak{b}^i_j + \eta^i_j$ (i subject, j voxel index)
- $\widehat{\mathfrak{b}}^i_j$: estimated effect size, $\widehat{\eta}^i_j$: within-subject variance

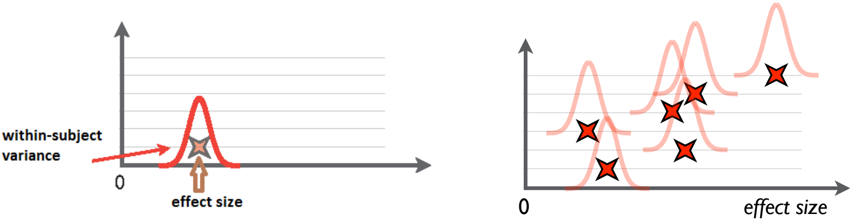

Figure 18: Estimated coefficient $\widehat{\mathfrak{b}}$ and the kernel density estimator of $\widehat{\mathfrak{b}} + \widehat{eta}$ for single subject (left) and multi-subjects (right). Figure modified from FEAT - FMRI.

Mixed-effects Model

▸ Cluster Activation

Consider the distribution of the effect size $\widehat{\mathfrak{B}} = \sum_{i=1}^{N} \mathfrak{b}_i$ from the wider population from which the subjects $i = 1, \ldots, N$ are sampled

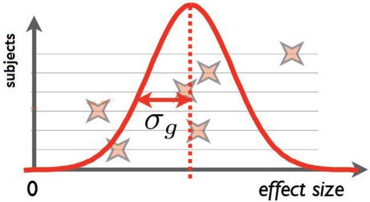

Figure 19: The kernel density estimator of $\widehat{\mathfrak{B}}$ for the entire population based on the analyzed sample; σ_g denotes the standard deviation of the population. Figure modified from FEAT - FMRI.

- Testing the sample mean: *is the group activated on average?*

B-Splines

▸ B-Splines

Univariate **B-spline** basis $\Psi = \{\psi_1(X), \ldots, \psi_K(X)\}^\top$ is a series of $\psi_k(X)$ functions defined by $x_0 \leq x_2 \leq \ldots \leq x_{K-1}$, K knots and order p, i.e. for $p = 2$ (quadratic)

$$\psi_j(x) = \begin{cases} \frac{1}{2}(x - x_j)^2 & \text{if } x_j \leq x < x_{j+1} \\ \frac{1}{2} - (x - x_{j+1})^2 + (x - x_{j+1}) & \text{if } x_{j+1} \leq x < x_{j+2} \\ \frac{1}{2}\left\{1 - (x - x_{j+2})^2\right\} & \text{if } x_j \leq x < x_{j+1} \\ x & \text{otherwise} \end{cases}$$

B-Splines

▸ B-Splines

- Knots K and order p has to be specified in advance (EV criterion); K corresponds to bandwidth

- In higher dimensions, for $dim(X) = d > 1$

$$\Psi = \{\psi_1(X_1), \dots, \psi_{K_1}(X_1)\} \times \dots \times \{\psi_1(X_d), \dots, \psi_{K_d}(X_d)\}$$

- Flexible and computationally efficient approach to capture various spatial structures

Experiment

▸ ID Experiment

- Incentive to be **rational**
  - Draw 1 ID task and multiply subject's choice by 100 EUR
    $9\% \times 100 = 9$ EUR
- Gaussian returns:
  - $\mu = 5\%, 7\%, 9\%, 11\%$
  - $\sigma = 2\%, 4\%, 6\%, 8\%$

Single Investment ▸ fMRI Experiment

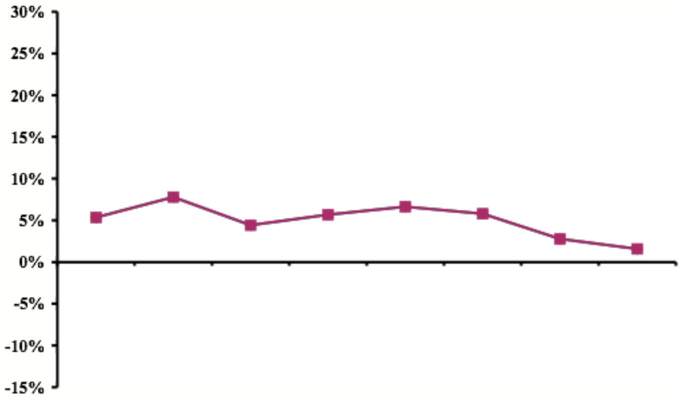

Figure 20: An example of return stream from single investment displayed to the subject during the experiment for 7 sec.; returns $r_i \sim \mathrm{N}(\mu, \sigma^2)$, here $\mu = 5\%, \sigma = 2\%$

Correlated Portfolio

fMRI Experiment

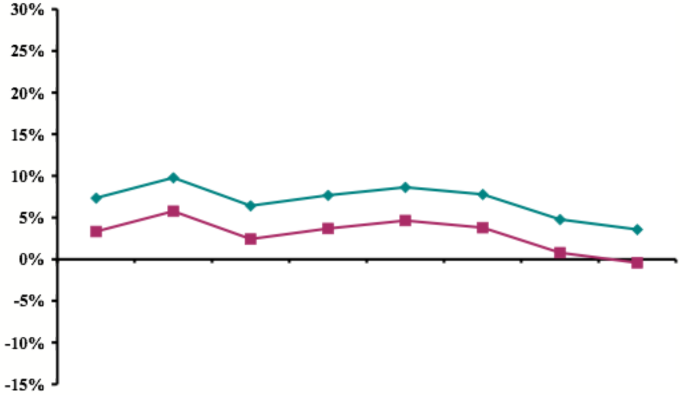

Figure 21: An example of return streams from correlated portfolio displayed to the subject during the experiment for 7 sec.; returns $r_i \sim N(\mu, \sigma^2)$, here $\mu_1 = 5\%, \mu_2 = 9\%$ and $\sigma = 2\%$

Uncorrelated Portfolio

▸ fMRI Experiment

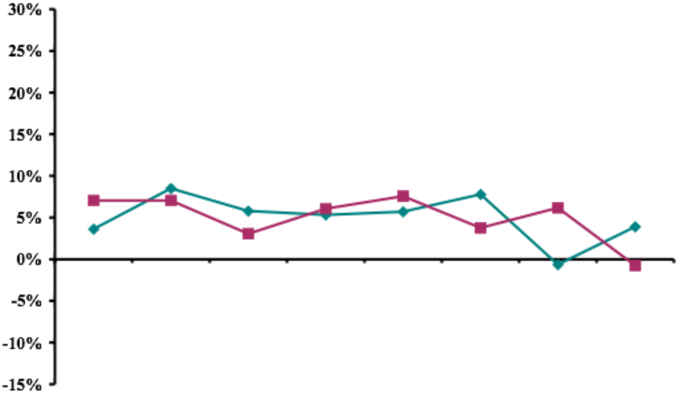

Figure 22: An example of return streams from uncorrelated portfolio displayed to the subject during the experiment for 7 sec.; returns $r_i \sim N(\mu, \sigma^2)$, here $\mu = 7\%, \sigma = 2\%$

Subject's Answers ▸ fMRI Experiment

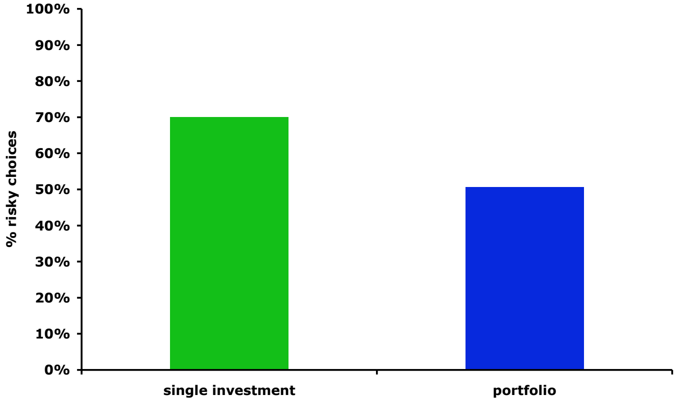

Figure 23: A proportion of risky choices selected by subjects for the single investment/portfolio (128/128 trials) setup averaged over all subjects.

aINS(left)

▸ aINS

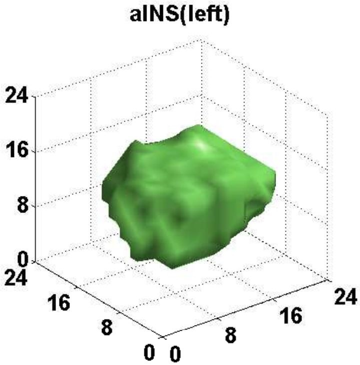

Figure 24: Derived aINS(l) regions for subject 1 (left) and 19 (right); axis are scaled in millimeters.

aINS(right)

▸ aINS

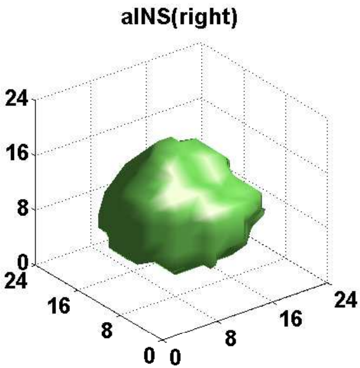

Figure 25: Derived aINS(r) regions for subject 1 (left) and 19 (right); axis are scaled in millimeters.

Cluster Activation: Results

	DSFM		Average		GLM	
aINS(l)	4.13	$(-34, 18, -8)$	4.08	$(-36, 18, -8)$	4.58	$(-32, 22, -12)$
		3×10^{-4}		4×10^{-4}		3×10^{-3}
aINS(r)	4.39	$(34, 24, -4)$	4.21	$(36, 18, -6)$	5.24	$(40, 22, -16)$
		6×10^{-6}		6×10^{-7}		3×10^{-7}
DMPFC	4.43	$(6, 24, 42)$	3.88	$(4, 24, 42)$	4.56	$(4, 24, 24)$
		2×10^{-9}		1×10^{-8}		3×10^{-7}

Table 3: Z-scores and p-values of activated "risk" clusters during the ID stimuli. The position of the cluster local maximum is denoted in the MNI (Montreal Neurological Institute) standard at 2mm resolution. Average stands for a mean value of each cluster (results of the Ncut parcellation with $K = 1000$). Analysis done in the FSL (FEAT/FLAME) software.

▸ aINS, ▸ DMPFC

Residual Analysis

▸ Cluster Activation

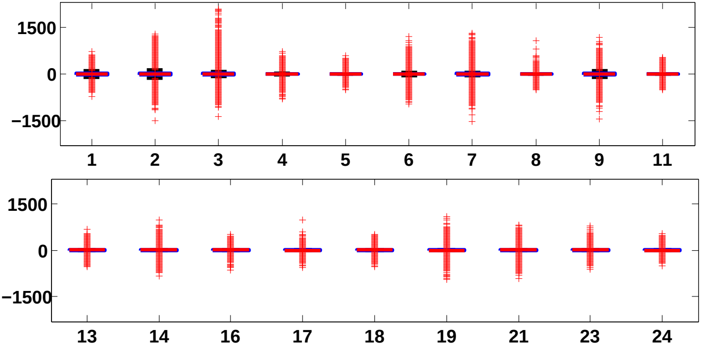

Figure 26: Boxplots of $\varepsilon^{i}_{aINS(l)}$ for all 19 analyzed subjects. Kurtosis exceeds 10

Residual Analysis

▸ Cluster Activation

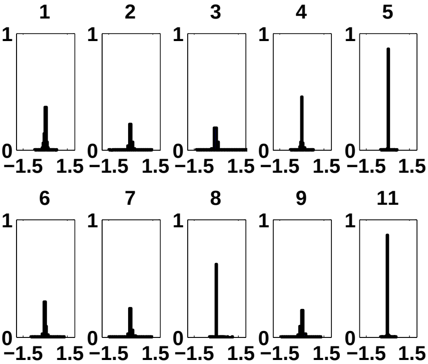

Figure 27: Histograms of $\varepsilon^i_{aINS(l)}$ for subjects $i = 1, 2, 3, 4, 5, 6, 7, 8, 9, 11$, respectively. Normality hypothesis (**KS test**) for standardized $\varepsilon^i_{aINS(l)}$ rejected for all subjects, $\alpha = 5\%$

Residual Analysis

▸ Cluster Activation

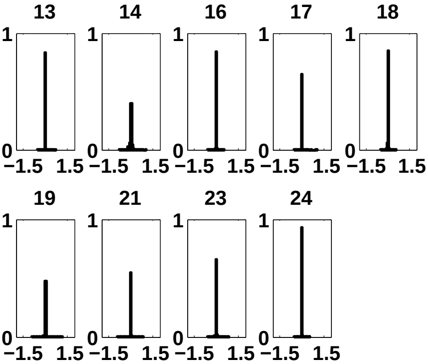

Figure 28: Histograms of $\varepsilon^{i}_{aINS(l)}$ for subjects $i = 13, 14, 16, 17, 18, 19, 21, 23, 24,$ respectively.

Residual Analysis

Cluster Activation

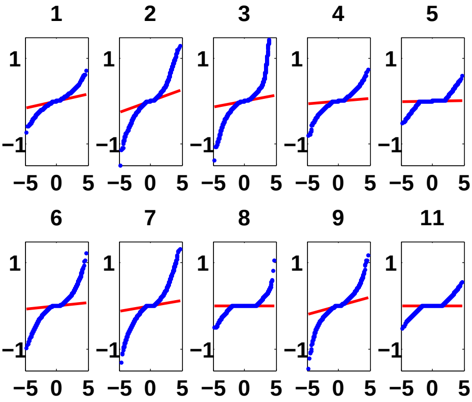

Figure 29: QQplots of $\varepsilon^{i}_{aINS(I)}$ for subjects $i = 1, 2, 3, 4, 5, 6, 7, 8, 9, 11$, respectively.

Residual Analysis

▸ Cluster Activation

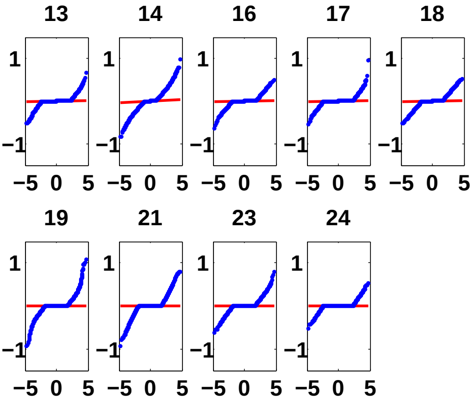

Figure 30: QQplots of $\varepsilon^{i}_{aINS(l)}$ for subjects $i = 13, 14, 16, 17, 18, 19, 21, 23, 24$, respectively.

ACF: DMPFC

DMPFC $\widehat{Z}$

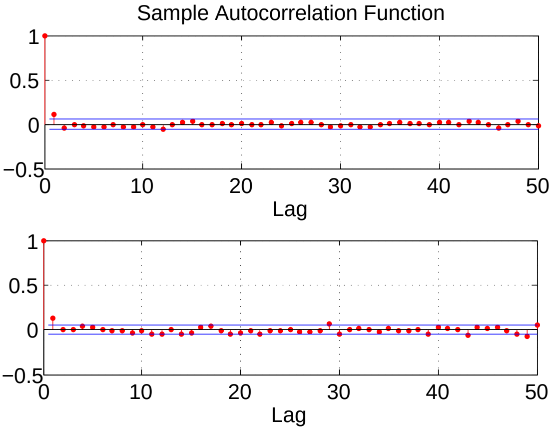

Figure 31: Sample autocorrelation function of **DMPFC** $\widehat{Z}$ for subjects 1 (top) and 19 (bottom), respectively.

ACF: aINS(l)

aINS(left) $\widehat{Z}$

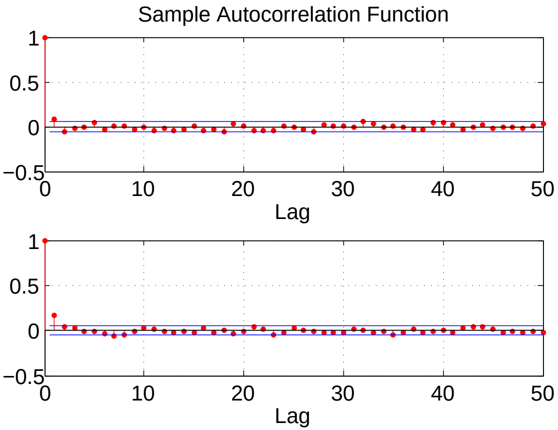

Figure 32: Sample autocorrelation function of **aINS**(left) $\widehat{Z}$ for subjects 1 (top) and 19 (bottom), respectively.

ACF: aINS(r)

aINS(right) $\widehat{Z}$

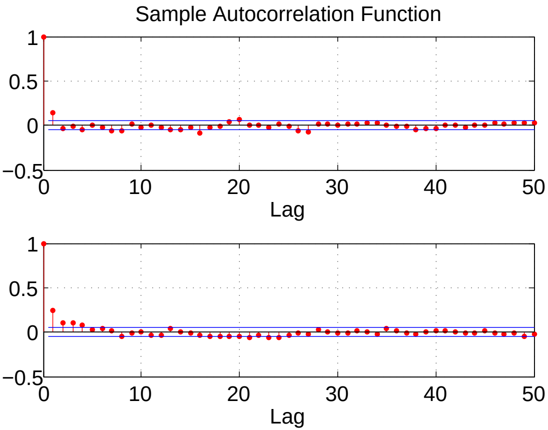

Figure 33: Sample autocorrelation function of **aINS**(right) $\widehat{Z}$ for subjects 1 (top) and 19 (bottom), respectively.

Simulation Study ▸ DSFM

$$Y_t = Z_t^\top m(X) + \varepsilon_t, \text{where:}$$

- Y_t is $6 \times 7 \times 6$, $t = 1, \ldots, 1400$ simulated BOLD
- $L = 1$ and $m(X) = m(x, y, z) = \|(x, y, z) - (6, 8, 6)\|$
- Z_t is a stimulus time series (HRF $\times 64$)

A) ε $(6 \times 7 \times 6 \times 1400)$ is a Gaussian **i.i.d noise**, $\mu = 0$, $\sigma = 6$

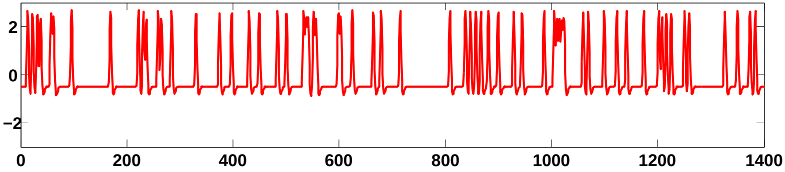

Figure 34: Stimulus time series derived by double Gamma hemodynamic response function $\times 64$.

Simulation Study ▸ DSFM

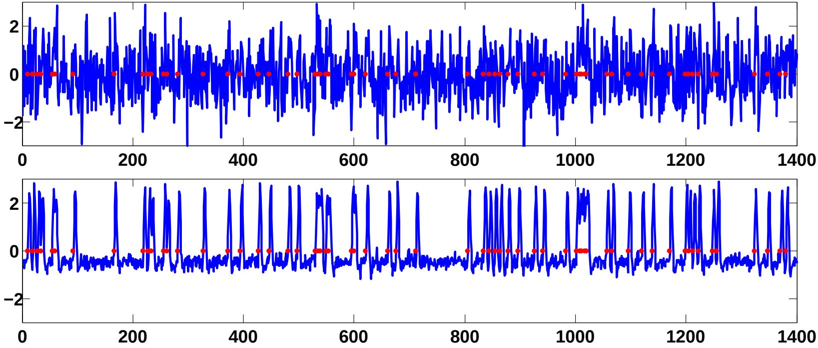

Figure 35: Time series of the simulated $(1, 1, 1)$ voxel $Y_{t,1}$ (top) and estimated $\widehat{Z}_t$ (bottom); red dots denote stimulus;$\mathrm{Corr}_t(\widehat{Z}_t, \text{stimulus}) = 0.98$.

Testing the activation: **Z-scores** for ▸ GLM and $\widehat{Z}_t$ higher than 100.

Simulation Study ▸ DSFM

$$Y_t = Z_t^\top m(X) + \varepsilon_t, \text{ where:}$$

B) ε $(6 \times 7 \times 6 \times 1400)$ is a Gaussian noise, $\mu = 0$, $\sigma = 6$, spatially smoothed by Gaussian kernel $(6, 6, 6)$mm (**correlated**)

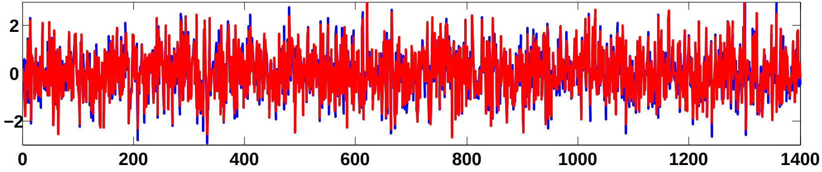

Figure 36: Simulated Gaussian noise for 2 vertical neighbor voxels (red and blue); $\mathrm{Corr}_t(\varepsilon_{t,1}, \varepsilon_{t,2}) = 0.97$.

Simulation Study ▸ DSFM

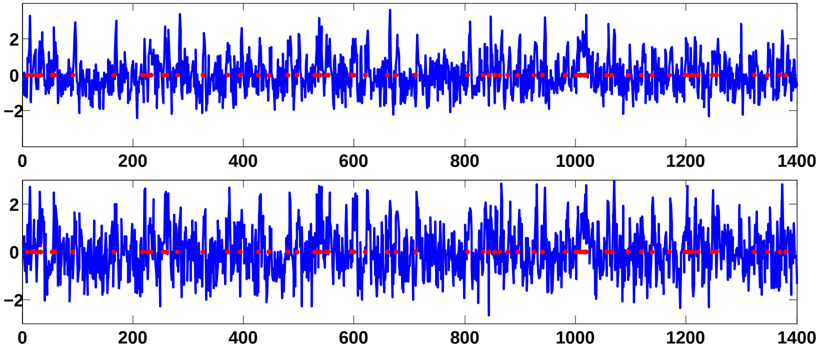

Figure 37: Time series of the simulated $(1,1,1)$ voxel $Y_{t,1}$ (top) and estimated $\widehat{Z}_t$ (bottom); red dots denote stimulus;$\mathrm{Corr}_t(\widehat{Z}_t, \text{stimulus}) = 0.60$. Testing the activation: **Z-scores** for GLM and $\widehat{Z}_t$: 30.79 and 27.96, respectively .

Correlation

Proximity Measure

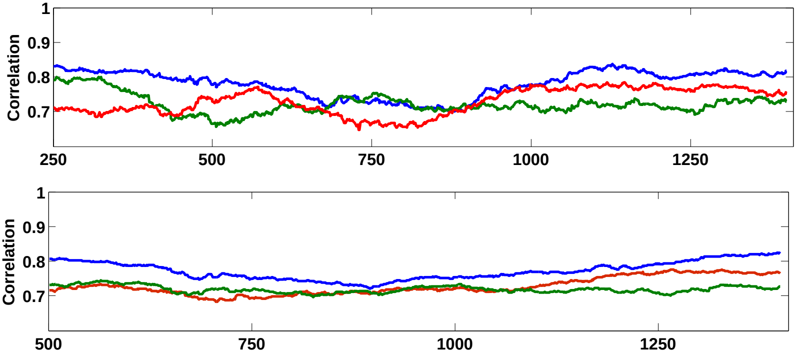

Figure 38: Time series of the correlation coefficient derived by the rolling window (250 top, 500 bottom) for the center voxel and: horizontal, vertical diagonal neighboring voxel for aINS(right) of subject 1.

Weights

▸ Weighted average reaction

- Optimal weights w defined as:

$$w^* = \operatorname*{argmin}_{\sum_{\tau=1}^{4} w_\tau = 1} \sum_{i=1}^{19} \left| \beta^i - \widetilde{\beta}^i \right|, \tag{5}$$

  where: $\widetilde{\beta}^i$ is predicted risk attitude and $\sum_{i=1}^{19} \left| \beta^i - \widetilde{\beta}^i \right|$ denotes absolute prediction error

- Solution found by Monte Carlo simulations with 10000 iterations